International Journal of Science and Research (IJSR)
ISSN: 2319-7064
Impact Factor (2018): 7.426

Optimizing Relative Height of Transformer Windings for Least Electromagnetic Forces

Deepika Bhalla[1], Raj Kumar Bansal[2], Hari Om Gupta[3]

[1]IK Gujral Punjab Technical University, Kapurthala, Punjab, 144 603, India

[2]Guru Kashi University, TalwandiSabo, Punjab, 151 302, India
J. P. Institute of Information Technology, Sector 128, 201 314Noida, India

Abstract: ***In distribution transformers helical winding is generally used for the LV side-that carries high current. The helical windings can be of multiple layers. The turn of a helical winding is wound in the axial direction along the helical line with an inclination A one-layer winding it starts at the bottom of the winding and finishes at the top. A two-layer helical winding turns are also wound along a helical line. The layer-one forms the outer/front coil and the layer-two forms the inner/back coil. The conductor passes from outer layer one to the inner layer two at the bottom both the start and the finish of the winding are at the top. The asymmetry caused by helical winding has an effect on the electromagnetic forces produced. Tappings also cause asymmetry. There is a need to find the the optimum relative height of LV and H V winding such the short circuit forces and the resulting mechanical stresses are least in a transformer having helical LV winding.***

Keywords: Electromagnetic forces, Finite element method, helical winding, Short circuit, Transformer.

1. Introduction

Power transformers are among the major apparatus in a power system, its' proper design along with monitoring of in-service behavior is necessary to avoid catastrophic failures and the resultant costly outages. Correct functioning of a transformer is vital to the system operations. When connected to a system of infinite fault capacity, the worst condition that can occur in practice is the current corresponding to the first peak of a three phase short circuit flowing through the windings. The interaction of the short circuit current with the flux produces electromagnetic forces and the stresses can be large enough to cause mechanical collapse of the winding, damage to the cellulose insulation, and deformation of the clamping structure. The mechanical stresses cannot be removed, but proper design can reduce them. The transformer must be designed to withstand mechanical stresses caused due to short circuit faults.To find the best design for a particular rating transformer so as to prevent failure is not possible because there is no agency that is involved in the activity for such analysis. The knowledge of the magnitude of forces would help the design engineer manage the mechanical stress caused during short circuit.

The mechanical stresses due to short circuit can damage the insulation, and deform the windings and core. For a particular design, if the region where excessive forces would occur is known then proper mechanical support and insulation can be provided. The proper design of windings and insulation can reduce the in-service failure of the transformer. The short circuit tests are carried out in specialized laboratories; these are expensive and time consuming to perform. There is thus a need of finding the forces in different regions of the transformer that would reduce the need of the expensive short circuit tests. With the increased current ratings of distribution transformers the short circuit capacity of the transformer needs utmost attention. The calculation of short circuit forces by numerical techniques such as Finite Element Method (FEM) can reduce the requirement of short circuit test.

Often it is seen that during short circuit in a transformer having helical windings, the yoke gets separated from the limb due to axial forces. The high forces in the end turn region cause mechanical damage to the insulation and windings. In case of repeated faults, the connection of the windings with the copper plate or bar comes off/ breaks.

FEM has been extensively used for calculating electromagnetic forces in transformers. The finite element analyses for computing forces in windings of a DT have been made, and results have been compared with those obtained by other research workers in the field [1, 2]. FEM has been used to study the impact of inrush current on mechanical stresses of high voltage power transformer's coil [3]. FEM has been used to review, and improve the winding support and tank wall of a power transformer [4]. FEM has also been applied to calculate the mechanical forces of current injection transformers, and it was concluded that the due to the low value of the ampere per turn in the High Voltage (HV) winding the forces produced are not destructive to its winding [5]. The electromagnetic forces on the windings of a three phase core type power transformer have been compared for 2D and 3D model [6]. FEM has also been used to compute the electromagnetic forces of a DT [7]. It has been found that the forces produced in 3D and simplified 2D asymmetric methods agree with each other, and the total forces in front and end view are quite close, and also the forces in the window region are more [8]. The FEM results from the 2D calculation of short-circuit forces on helical type Low Voltage (LV) windings are very close to 3D calculation except for the forces in the clamping structure [9]. Safety factors for radial and axial force during short circuit in a power transformer using the results of FEM have been found [10]. The electromechanical forces due to short circuit in a dry type transformer was studied by dividing the windings into sections, it was the first attempt

to find the short circuit forces in four sections along the circumference [11]. As per literature survey the forces found by FEM are in good agreement with analytical and experimental values [12].

FEM application for the study of helical winding initiated in 2001, the effect of transposition of double helical winding was observed [13]. The circumferential displacement in helical winding was studied and it was found that as the helical angle increases, the circumferential forces and displacement increase and maximum stresses occur in the ends of the winding[14].Short circuit axial forces in helical winding of one layer and two layer helical winding have been calculated [15,16]. However, work on finding the optimum relative height of the LV and H V winding so the short circuit forces and the resulting mechanical stresses are least so as to have reliable operation of transformer need to be undertaken.

2. Coupled field for Short Circuit Electromagnetic Forces in Windings

2.1 Electromagnetic Forces:

The rated current of LV inner winding is very large, and it has a small number of turns, while HV outer winding has less current and large number of turns. The currents in the two winding are in phase opposition to each other; thus, the force is of repulsion type, such that the distance between the two windings increases. The turns within a winding carry current in the same direction because of which they experience force of attraction, thus, this force compress the winding in the axial direction. The conductors of the winding lie in the region of the magnetic leakage flux and as per the Fleming's left hand rule, they experience a force that has a direction perpendicular to the direction of the current flow and the leakage flux.

The directions of the electromagnetic forces in a transformer are illustrated in Figure 1. In symmetrically placed windings, the axial component of the leakage flux density (Ba) interacts with current in the winding, producing radial force. This radial force is responsible for the repulsion between the HV winding and LV winding. The radial flux component (Br) interacts with the winding current to produce axial force.

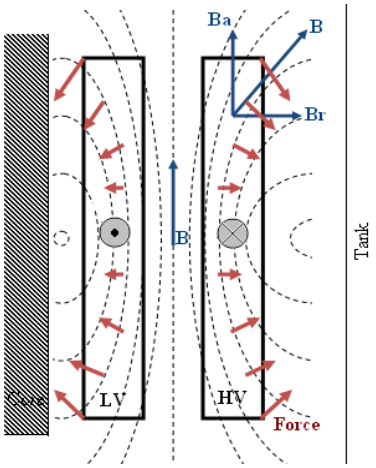

Figure 1: Distribution of electromagnetic forces in transformer for symmetrically placed windings

This axial force act in such a way so as to produce axial compression in the winding, under ideal conditions. Axial force predominates radial force. In case the current density increases the electromagnetic forces also increase. These electromagnetic forces produce mechanical stresses in transformers.

The mechanical forces in the transformer winding conductors can be classified into two types namely external forces and internal forces. The external forces are due to interaction of current in different windings and the internal forces are due to interaction of currents within a winding. The external forces are directed towards the radius and tend to increase the distance between the windings, they are called radial forces. For concentric windings, the radial force tends to burst the outer HV winding and crush the inner LV winding. Also when the windings having equal axial height and uniformly distributed mmfs, the internal forces are called axial forces. For electromagnetically balanced windings, the axial forces are of compressive nature and have a tendency to reduce the height of the winding.

On assuming that, the forces of interaction between windings pass through the centre of gravity of their longitudinal section, and their direction is along the straight line joining them. Figure 2 shows the forces of interaction between asymmetrically placed windings; in such a case the inner LV winding moves upwards and the outer HV winding moves downwards. Under such condition, the axial forces are both due to external and internal forces. Asymmetries may cause the external axial force to act in the same direction of the internal axial force or may be in the opposite direction. This would decrease or increase the pressure on the spacers. When the axial height of the LV and HV windings are unequal or in case the mmfs are non-uniformly distributed along the height of the winding, the forces that are produced are such that they increase the asymmetry. The effect of such forces is is studied by coupled field theory.

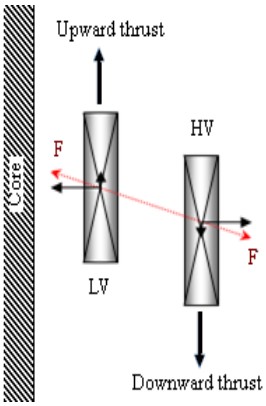

Figure 2: Forces of interaction between asymmetrically placed windings

2.2 Coupled Field Theory

The differential equation of the vector field defined along with the boundary Γ of the domain X is given by

$$D\Phi(P,t) = f(P,t) \qquad (1)$$

where, D is a linear differential operator, $\Phi$is the unknown function to be determined which may be a vector or a scalar field, f is the forcing function of the position, $P(x,y,z)$in

space, and of the time, t. In an electrostatic problem the scalar electric potential V is indicated by Φ and its distribution is described by Poisson Equation [17]. The forcing function is the distribution of free charge density $f = \rho$ and the equation (1) is rewritten as

$$-div\,(\varepsilon\ grad\ V) = \rho \qquad (2)$$

The behavior of the function Φ on the boundary Γ is expressed by the boundary conditions. The boundary conditions are of two types namely Dirichlets's condition and Neumann's condition. The Dirichlet's condition is given when a given value of Φ is assigned on the boundary Γ. The Neumann's condition is given when value of the derivative of Φ normal to the boundary Γ is assigned.

If a portion of the boundary is Γ_1, then the Dirichlet's boundary condition on this boundary for homogenous condition is $\Phi = 0$, and for nonhomogenous condition it is, $\Phi = \Phi_i$. If the remaining portion of the boundary is Γ_2, then Neumann's boundary condition for homogenous condition is $\frac{\partial \Phi}{\partial n} + k\Phi = 0$,and for nonhomogenous condition it is, $\frac{\partial \Phi}{\partial n} + k\Phi = \Phi_g$.

The field problems can be solved by three methods, namely Galerkin's Method or the Classic Residual Method, Rayleigh-Ritz's method or the Classic Variational Method and Finite Element Method. All the above methods approximate the function Φ as closely as possible and thus define a function Φ^*that is commonly expressed as a linear combination of the basic functions and is given by

$$\Phi^*(P,t) = \sum_{j=1}^{N} \Phi_j v_j\,(P,t) \qquad (3)$$

where Φ_j are unknown coefficients that are determined during computation and v_j are interpolation functions, at times referred to as base or expansion functions.

The classical methods take the entire analysis domain into account and the interpolation functions are defined on the entire domain. The FEM divides the entire domain into subdomains. Φ^* is a combination of the functions v_j that are defined in the subdomains. This results in the subdomains of very small dimensions and a very simple function, v_j.
The inner product between two functions Φ and $\varphi$for volume τ is defined as

$$\langle \Phi, \varphi \rangle = \int_{\tau} \Phi \tilde{\varphi}\, d\tau \qquad (4)$$

where ˜ indicates the complex conjugate. The properties of additively and the product by a constant are satisfied, since the inner product is a linear operator, thus

$$\langle \Phi_1 + \Phi_2, \varphi \rangle = \langle \Phi_1, \varphi \rangle + \langle \Phi_2, \varphi \rangle \qquad (5)$$
$$\langle \alpha\Phi, \varphi \rangle = \alpha \langle \Phi, \varphi \rangle \qquad (6)$$

It is essential that the differential operator D is positive and is defined as

$$\langle D\Phi, \varphi \rangle = \begin{cases} > 0, & \Phi \neq 0 \\ = 0, & \Phi = 0 \end{cases} \qquad (7)$$

and to change the argument of the operator D within the operation of the inner product if possible, i.e

$$\langle D\Phi, \varphi \rangle = \langle \Phi, D\varphi \rangle \qquad (8)$$

2.2.1 Galerkin's Method

This method directly deals with the differential equation (1). To solve the field problem, the residual of this differential equation is reduced, so it is also referred to as the classic residual method. It is assumed that: the function Φ^* that better approaches the exact solution Φ corresponds to a residual that is equal to zero in the entire domain of analysis.

$$\text{The residual is } r = D\Phi^* - f \qquad (9)$$

In the residual method, the weight functions are introduced, this forces the integral of the residuals weighed by w_i to be zero over the domain volume τ_X. The condition that is forced is given as

$$R_i = \int_{\tau_X} w_i\,(D\Phi^* - f)\, d\tau = 0 \qquad (10)$$

In this method, the weigh functions are chosen equal to the interpolating function *i*.e.

$$w_i = v_i \quad i = 1, 2, 3, \ldots, N \qquad (11)$$

On using the approximation of equation (3), equation (10) becomes

$$R_i = \int_{\tau_X} v_i\, D\left(\sum_{j=1}^{N} \Phi_j\, v_j\right) - v_j f d\tau. \qquad (12)$$
$$i = 1, 2, 3, \ldots, N$$

From the above equation the system equations that are developed are expressed by

$$[SS][\Phi] = [T] \qquad (13)$$

where $[\Phi]$ is a column vector of unknown coefficients Φ_i, $[SS]$ is a vector matrix which depends upon the interpolating functions, the elements of which are given by

$$s_{ij} = \frac{1}{2}\int_{\tau_X} \left(v_i D v_j + v_j D v_i\right) d\tau \qquad (14)$$

[T] is a column vector whose elements depend upon the forcing function which is given by

$$t_i = \int_{\tau_X} v_i\, f d\tau \qquad (15)$$

2.2.2 Rayleigh-Ritz's Method

The Rayleigh-Ritz method uses an integral approach to solve the field problem. A variational function is built from the differential equation (1)such that its minimum corresponds to the solution. The field problem is solved when the field equation and the boundary conditions match [17]. The minimum of the variational function that corresponds to the solution of equation (1) is expressed by

$$F(\Phi) = \frac{1}{2}\langle D\Phi, \Phi \rangle - \frac{1}{2}\langle \Phi, f \rangle - \frac{1}{2}\langle f, \Phi \rangle \qquad (16)$$

If function Φ is substituted by Φ^* of equation (3)and $v_i$is defined in the entire domainX. On substituting (3) in (16) and equating to zero the derivatives of the variational function $F$with respect to unknown coefficients Φ_i, i.e.

$$\frac{\delta F}{\delta \Phi_i} = 0 \qquad i = 1, 2, 3, \ldots, N \qquad (17)$$

a system of linear quations is obtained. The property defined by equation (8)needs to be valid, hence the matrix vector $[SS]$ is symmetrical and the system is identical to that obtained by the residual method [17].

2.2.3 Finite Element Analysis

Finite Element Method (FEM), a numerical technique can be used for computing electrical and magnetic fields. Field solutions with time varying fields and materials that are non-homogenous, anisotropic or nonlinear can be obtained using it. In this method, the analysis domain is divided into elementary subdomains called finite elements and the field equations are applied to each subdomain. The method is based on the solution of Maxwell's equations applied to the structure under study.

The advantages of study of electromagnetic field distribution using FEM include precise local analysis, highlighting dangerous field gradient, calculation of magnetic field strength, magnetic saturation, etc. The FEM also gives a good estimation of the electromagnetic device under analysis and substantially reduces the number of prototypes of device under study. The drawback of FEM is that the solutions are approximate on account of it being of numerical nature. If not applied correctly, it might produce inaccurate results and the computation time required may be long [17].

The finite element analysis uses the following steps:
Step1:Partition of the domain
Step 2: Selecting the interpolating functions
Step 3: Formulation of the system to solve the field problem
Step 4: Solution of the field problem

2.3 FEM for Computing Forces in Winding

The electromagnetic forces in transformer windings can be found using finite element method (FEM). To reduce the size of the field problem the analysis is generally carried out in sections having geometric and magnetic symmetries. The flux lines are symmetrical in regard with the vertical axis and horizontal axis. The boundary conditions need to be applied on the symmetry lines.

The equivalent circuit of a lossless transformer is shown in Figure 3. The winding resistances, core losses, and saturation are not considered. For a transformer, the voltage equations are given by

$$v_1 = \frac{d\lambda_1}{dt} = L_1\frac{di_1}{dt} + M\frac{di_2}{dt} \quad (18a)$$

$$v_2 = \frac{d\lambda_2}{dt} = M\frac{di_1}{dt} + L_2\frac{di_2}{dt} \quad (18b)$$

where $v_1, v_2, i_1, i_2, \lambda_1$ and λ_2 are the voltages, currents, and flux linkages at the two terminals. The sign convention is such that the positive direction of the currents is against the voltages in both terminals. $L_1, L_2,$ and M are the self and mutual inductances and are constant since it is assumed that there is no saturation and the inductances are constant. The flux linkages are expressed as $\lambda_1 = L_1 i_1 + Mi_2$ and $\lambda_2 = L_2 i_2 + Mi_1$

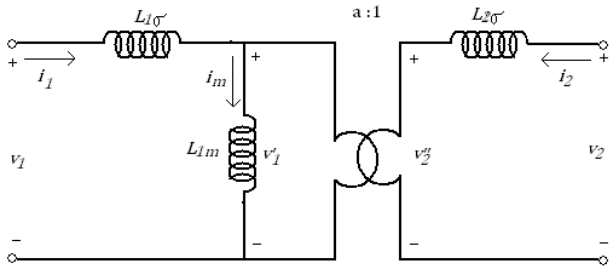

Figure 3: Equivalent circuit of the real transformer

The self-inductances are

$$L_1 = L_{1\sigma} + L_{1m} \quad (19a)$$

$$L_2 = L_{2\sigma} + L_{2m} \quad (19b)$$

such that $L_{1m}L_{2m} = M^2$

where, $L_{1\sigma}, L_{2\sigma}$ are leakage inductances referred to primary and secondary winding. An ideal transformer has a perfect coupling of L_{1m}, L_{2m} and M. The transformation ratio "a" is given by

$$a = \frac{L_{1m}}{M} = \frac{M}{L_{2m}} \quad (20)$$

The choice of the transformation ratio is useful to impose the current sources in finite element analysis of the leakage inductances. To compute the magnetizing inductances a simulation is carried out that corresponds to the open circuit test. In the test the primary winding is fed rated voltage at rated frequency and the primary current and induced secondary voltage are measured. For simulation, the primary winding current is imposed as the field problem source and the corresponding voltages for the two windings are computed. The magnet vector potential is derived so as to obtain the components of magnetic flux density in the core. Assuming the material to be linear, the stored magnetic energy corresponding to the current feeding the primary winding, it is computed as:

$$w_m = \frac{1}{2}\boldsymbol{B}.\boldsymbol{H} = \frac{1}{2}\mu_{Fe}H^2 \quad (21)$$

The magnetic energy stored in the transformer can be computed on integrating the energy density over the entire volume. If the net iron length of the transformer is L_{fe}, then the energy in the transformer is

$$W_m = L_{fe}\int_S \frac{1}{2}\mu_{Fe}H^2 dS \quad (22)$$

where, B is magnetic flux density, H is magnetic field strength, S is the total surface of the domain , and μ_{Fe} is the permeability of the core.

The main flux is found by integrating the component of the flux density that is normal to the core section over the same surface. For a core type transformer, the magnetic flux at no-load is:

$$\Phi_0 = L_{Fe}\int_l \boldsymbol{B}.\boldsymbol{n}dl \quad (23)$$

where L_{Fe} is net iron length and $\boldsymbol{n}$ is a normal unit vector to the surface.

The flux linkages are found by integration of the magnetic vector potential A_z over the surface of the equivalent sections/bars that form the primary winding

$$\Lambda_{10}= N_1 L_{Fe}\left(\frac{1}{S_{cu1}}\int_{S_{cu1+}}^{\square\square} A_z dS - \int_{S_{cu1-}}^{\square\square} A_z dS\right) (24a)$$

$$\Lambda_{20}= N_2 L_{Fe}\left(\frac{1}{S_{cu2}}\int_{S_{cu2+}}^{\square\square} A_z dS - \int_{S_{cu2-}}^{\square\square} A_z dS\right) (24b)$$

where S_{cu1+} , S_{cu1-} and S_{cu2+} and $S_{cu2-}$are the surface of the equivalent copper bar where the current direction is positive and negative in the primary and secondary winding respectively, and also $S_{cu1+} = S_{cu1-} = S_{cu1}$ and $S_{cu2+} = S_{cu2-} = S_{cu2}$. $N_1$and $N_1$are the number of turns of the primary and secondary winding.

The induced EMF's in the primary and secondary windings are

$$E_{10} = \omega\Lambda_{10} \quad (25a)$$
$$E_{20} = \omega\Lambda_{20} \quad (25b)$$

where Λ_{10} and $\Lambda_{20}$are the maximum values of flux linkages of primary and secondary windings. $E_{10}$and $E_{20}$are EMF of primary and secondary windings. The operating frequency of the transformer is $\omega = 2\pi f$.
All simulations are carried out considering the maximum value of the current.

The leakage inductances are given by:

$$L_{1\sigma} = \frac{\Lambda_{10}}{I_{10}} \quad (26a)$$
$$L_{2\sigma} = \frac{\Lambda_{20}}{I_{20}} \quad (26b)$$
$$M = \frac{\Lambda_{20}}{I_{10}} \quad (26c)$$

The current densities are given by:

$$J_{1z} = \frac{N_1 I_1}{S_{cu1}} \quad (27a)$$
$$J_{2z} = \frac{N_2 I_2}{S_{cu2}} \quad (27b)$$

$N_1$and $N_2$are the number of turns in the primary and secondary winding. The Lorentz's force in the coil along the x-axis and y-axis is:

$$F_x = -l_{avg}\int_{Scu1}^{\square\square} J_z B_y dS \quad (28a)$$

$$F_y = -l_{avg}\int_{Scu1}^{\square\square} J_z B_x dS \quad (29b)$$

where J is the current density vector and B_x, B_y are field density vectors and l_{avg} is the average length of the iron path.

The interaction between current density and leakage flux density generate electromagnetic forces within a transformer. In a transformer having concentric windings, the flux bends towards the core at the end of the windings making the return path of the flux shorter. This phenomenon is observed both at the top and bottom ends of the windings [102].

2.3 Short Circuit Current in Transformer

When a transformer is connected to a system of infinite fault capacity, the worst condition that can occur in practice is the current corresponding to the first peak of a three phase short circuit flowing through the winding. The maximum value of short circuit current I_{sc} (amps)is given by the expression

$$I_{sc} = \frac{\sqrt{2} \times k \times MVA \times 10^6}{\sqrt{3} \times V_1 \times e_z} \quad (30)$$

where, k is the asymmetry factor, e_z is fractional per unit impedance voltage and V_1 is the primary voltage. The value of $\sqrt{2} \times k$ is calculated as per clause 16.11.2 of IS-2026 [18], which is identical to IEC standard 60076 [19]. The impedance voltage e_z depends upon the tapping position, so as to calculate the forces accurately the value of impedance corresponding to the tapping position needs to be considered [20].

The short circuit current has a steady-state alternating component at the fundamental frequency and an exponentially decaying current. The force experienced by a winding is proportional to the square of the short circuit current. The force has four components, there are two alternating components and two unidirectional currents. One of alternating component is at the fundamental frequency, and the other at double the fundamental frequency, the double frequency component of current is of a constant but smaller value. The other two components of force are unidirectional; one is constant and the other is decreasing with time. With a fully offset current, the fundamental frequency component of force is dominant during the initial cycles [21].

The first peak of the short circuit current is of very large magnitude; it is this part of the current wave that is important from the point of view of dynamic stability and the mechanical strength of the transformer. If the transformer can withstand the force at this point of time, then it has the ability to withstand the forces generated in the subsequent part of the current waveform. The subsequent part of the current waveform is important from thermal stability point of view.

When a three phase short circuit occurs there is a heavy concentration of electromagnetic fields in the core window and maximum failure in core type transformer very often occur in this region. The windings on the central limb are subject to higher forces. There is a considerable variation of forces along the winding circumference [106].

3. Design, Modelling and Simulation

3.1 Design

The design of 630kVA, 11000/433kV power distribution transformer considered for the study of short circuit forces are given in Table 1[15,16], and the other parameters and dimensions of the core are height 195mm, diameter 200mm, leg center 350mm, window height 440mm and stacking factor 0.97 and core material M4, and maximum flux density is 1.68 T. The dimensions of the winding and core are shown in figure 4.

3.2 Modeling of Windings

3.2.1 One Layer Winding

The LV winding of the transformer has 23 turns. The conductor used has 2 strips along the width and 5 strips along the depth. Each turn coils up in a clockwise direction, the helical angle of which is found from the pitch and mean circumference. As the winding coils up the change in the symmetry is considered for thirteen vertical sections, the entire circumference gets divided into twelve equal sectors. When there is no asymmetry, each vertical section has a height of 398mm (height of winding) and width of 23.75 mm and 32mm for LV and HV winding respectively. The axial and radial forces (N) are calculated per unit depth (mm) in z-direction; for the rectangular bar/surface (vertical section of the winding) of 398mm X 23.75mm for LV winding and 398mm X 32mm for HV winding using FEM. The average radial force in the LV winding is found by taking the average value of the radial forces in the thirteen sections along the circumference. The net axial force in LV winding is the sum of the axial forces in the twelve sectors. The force in each sector is the average value of force between two adjacent sections multiplied by ($\pi D_m/12$) [12,15].

Table 1: Specifications of 630kVA, 3 Phase Power Distribution Transformers

Parameters	Winding		
	HV	**LV**	
Type of coil	cross-over	One layer-helical	Two layer-helical
No of coils per phase	2	1	1
No of turns per phase	1062	23	23
Conductor size (bare)	Diameter: 2.850	6.70X4.25 X10	10.02X4.70 X6
Conductor size covered	3.150	7.10X4.65	10.42X5.10
Conductor placement	-	2WX5D	3WX2D
Inner diameter of coil (mm)	275.5	207	207
Axial length of coil (mm)	398	398	398
No of turns per coil	531	23	23
No of layers	9	1	2
No of turns per layer	59	23	11.50
Outside diameter of coil(mm)	339.5	254.5	254.5
Voltage (V)	11000	433	433
Yoke clearance	21.5	11	13
Inter phase connections	Delta	Star	Star

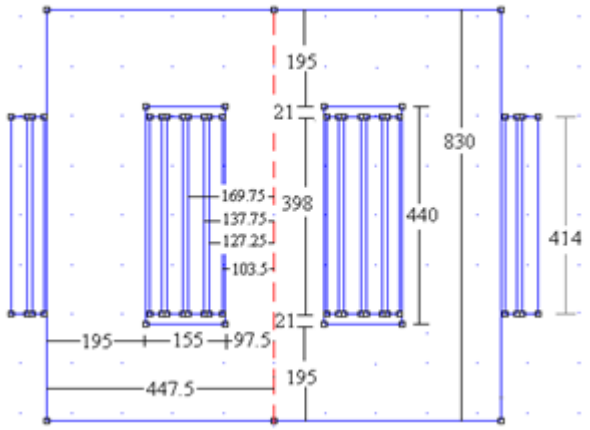

Figure 4: Dimensions (mm) of winding and core for equal effective height of one layer LV and HV windings

The average radial force in the HV winding is found by taking the average value of the radial forces in the thirteen sections along the circumference. To compute the net axial force in the HV winding, the average value of the axial force of thirteen sections is multiplied by the mean circumference.

So as to find the optimal height of LV winding when the stresses in both windings and end turn are least the effective height of LV winding is varied in steps of ±1% to that of the HV winding.

To study the effect of center tapping, 10% of the middle of the HV winding is removed. The thinning of LV winding adjacent to the tapped region has not been taken into account.

3.1.2Two Layer Winding

The two-layer winding starts and finishes at the top. The inner layer conductor passes to the outer layer at the bottom, so an additional turn is provided. Turns 1-12 constitute the inner layer and turns 13-24 constitute the outer layer. The start of turn-1 of the inner layer and end of turn-24 of the outer layer are connected to the line terminal. Turn-1 and turn-24 are at the top, and turn-12 and turn-13 are at the bottom of the winding. The conductor used has 3 strips along the width and 2 strips along the depth. The helical angle is found from the pitch and the mean circumference. As the winding coils up there is change in the symmetry of outer and inner layer, it is considered for thirteen vertical sections. The inner layer turns coil up in the clockwise direction, (from section-1 towards section-13) and the outer layer turns coil up in anticlockwise direction from section-13 towards section-1). The entire circumference gets divided into twelve equal sectors. When there is no asymmetry, each section has a height of 398mm (height of winding) and width of 23.75 mm and 32mm for LV and HV winding respectively. The axial and radial forces (N) are calculated per unit depth (in z-direction) for the rectangular bar/surface (vertical section of the winding) of 398mm X 11.875mm each for inner and outer layer of LV winding and 398mm X 32mm for HV winding. The radial force and axial force in per unit depth in these two rectangular bars are computed the space between the inner and outer layer is ignored.

The average radial force in each layer of LV winding is found by taking the average of the radial forces in the thirteen sections of the respective layer along the circumference. The net axial force in LV winding is the sum of the axial forces in the twelve sectors of both the layers taken together. The force in each sector is the average force between two adjacent sections multiplied by ($\pi D_m/12$). The average radial force in the HV winding is found by taking the average of the radial forces in the thirteen sections along the circumference. To compute the net axial force in the HV winding, the average value of the axial force of thirteen sections is multiplied by the mean circumference [12,16].

The axial height of the HV (hHV) is kept fixed (398 mm) while the effective height of LV (hLV) is varied in steps of ±1% for one layer and +1% for two layer helical LV windings. So as to study the effect of asymmetry caused by tapping, the center +10% of HV is tapped. Forces are found for both without and with tapping of HV winding.

To study the effect of tapping, 10% of the middle of the HV winding is removed. The thinning of LV winding adjacent to the tapped region has not been taken into account in this study.

3.3 Simulation

The software Finite Element Method Magnetic (FEMM) version 4.2 has been used to compute the short circuit forces. FEEM 4.2 considers current driven magnetics. The complete section of the transformer is used for simulation of the forces and Dirichlet boundaries are used [22]. In the 2-D modeling of the transformer, the cross section of the core and the winding is considered, and the per unit depth (z-direction) in mm is taken into account. Rectangular bars/sections are used which are taken to be equal to the entire coil of the winding. The core section is taken to be circular, and all the results are taken for the window region.

The magnetostatic simulation is carried out by feeding constant currents into the windings, I_1 in the primary and $I_2 = -I_1(N_1/N_2)$ in the secondary, where N_1 and N_2 are the number of turns in the primary and secondary. The maximum value of short circuit current I_{sc} is found using equation (30) value of asymmetry factor k is taken as 1.8. To simulate the electromagnetic fields at the time the fault occurs, it is taken that the first peak of the symmetrical current passes through the central/middle limb. The core is assumed to be linear and with constant permeability.

Problem definition: Type: Planar, Unit length: millimeters, Frequency: 50 Hz, Depth: 1 mm, Solver precision: 1e-008, Minimum angle: 30°, AC solver: Successive precision

4. Material Properties

Core: Linear region, permeability in x-direction: 7000, permeability in y-direction 7000, lamination thickness: 0.27mm, Lamination fill factor 0.97. HV winding: permeability in x-direction: 1, permeability in y-direction:1, electrical conductivity: 58MS/m, number of strands:1, strand diameter : 2.85mm. LV winding: permeability in x-direction: 1, permeability in y-direction:1, electrical conductivity: 58MS/m, number of strands:1, strand diameter : 18.97mm

In this study, the values of the computed forces in the LV and HV winding are the forces exerted in the bar on the right side of the central limb. Hence, the negative values of radial force are directed towards the central limb of the core and are compressive. The positive values of radial force are directed towards the tank and are of bursting nature. The negative values of axial force are in downward direction, towards the lower yoke and are of compressive nature. The positive values of axial force are in the upwards direction, towards the upper yoke, hence are tensile in nature.

After design and simulation the flux distribution when the windings are symmetrical with only central limb energized (Section-8), with center tapping under short circuit condition is shown below in figure 5.

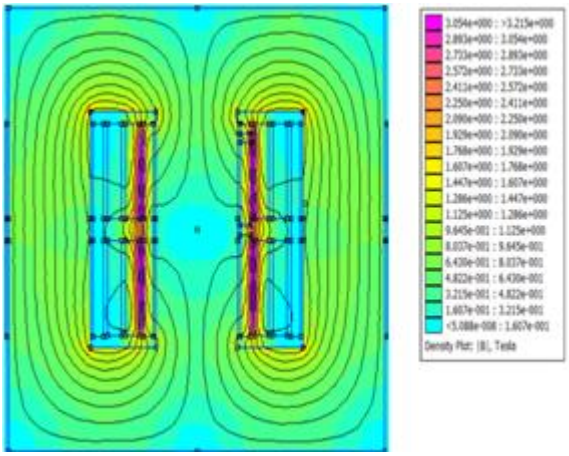

Figure 5: Flux distribution when central limb is energized

5. Results and Analysis

5.1 Short Circuit Forces in One Layer LV Winding

5.1.1Average Radial Force: The average value of the radial force in LV winding directed towards the core for all the cases are shown in Figure 6.As the effective height of LV winding compared to HV winding is increased (Case-7 to Case-11) there is a decrease in the magnitude of radial force. As the effective height of LV winding compared to HV winding is decreased (Case-5 to Case-1) the radial forces increase. The presence of tapping reduces the value of average radial force marginally, with relatively more effect for Case -1 and least for Case-11.

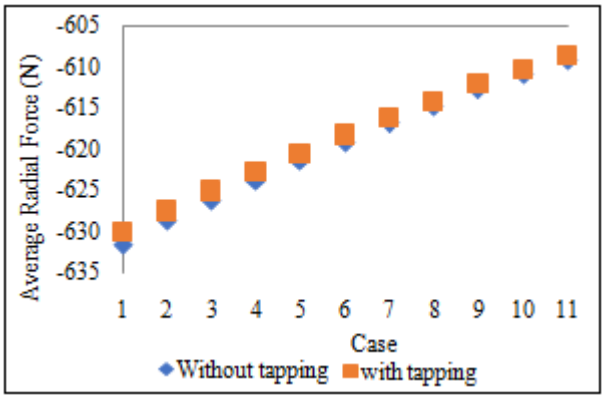

Figure 6: Average radial force in one layer LV winding for different effective axial height of LV winding keeping the height of HV winding fixed

5.1.2 Net Axial Force: Due to the helical nature at the start of the winding in section-1 the force acts in a downward direction and as the helix climbs up the force acts in an upward direction in section-13. Figure 7gives the net axial force in one layer LV winding for different cases. In case of untapped winding the net axial force in the one layer LV winding acts downward and is exerted on the lower yoke for Case-1 to Case-6, but as the relative height of the one layer LV becomes more than that of HV winding the net axial force acts upwards and is exerted on the upper yoke. The least magnitude net axial force in upwards direction is observed for Case-8. In case of tapped winding, the net force is always directed towards the upper yoke and of large magnitude. The transformer is uneconomical when the

effective height of the one-layer LV winding is less than HV winding; hence, LV windings with an effective height less than the height of HV winding are not preferred.

5.2 Short Circuit Forces in Two Layer LV Winding

5.2.1Average Radial Force: The figure 8 gives average radial short circuit force in two layer LV winding for different effective axial height of LV winding keeping the height of HV winding fixed. As the effective height of two layer LV winding becomes more than the height of HV winding the magnitude of radial force decreases marginally. The presence of tapping negligibly reduces the average radial force.

5.2.2 Net Axial force: The figure 9 gives net axial short circuit force in two layer LV winding for different effective axial height of LV winding keeping the height of HV winding fixed. For untapped winding the axial force in LV winding acts in downward direction towards the lower yoke. The average valve in the sections for a particular case, of the downward force varies from 26N to 31N (per unit depth in z-direction) for different cases. Thus, the magnitude of net axial force acting in a downwards direction for untapped winding is least force Case-6 and maximum for Case-11.

For tapped winding the axial force in LV winding acts in a downward direction towards the lower yoke. The magnitude of net axial force acting in downwards direction for tapped winding is least force Case-6 and maximum for Case-11.

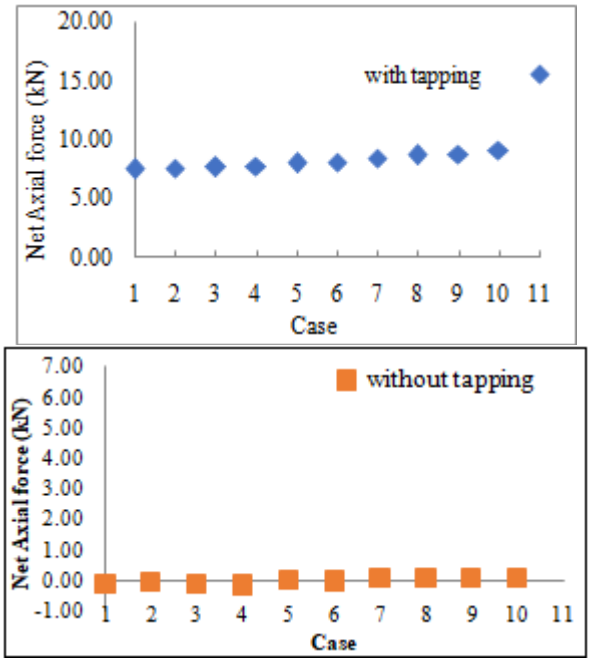

Figure 7: Net axial force in one-layer LV winding for different effective axial height of LV winding keeping the height of HV winding fixed

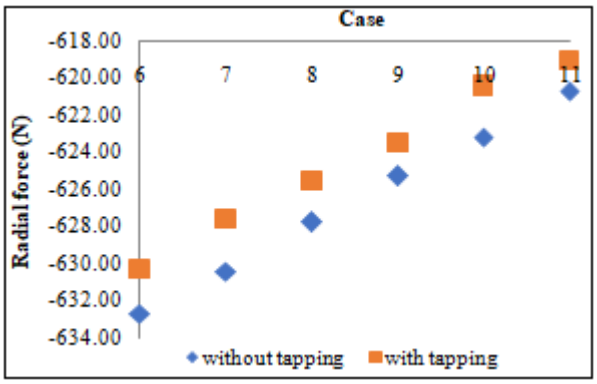

Figure 8: Average radial force in two-layer LV winding for different effective axial height of LV winding keeping the height of HV winding fixed

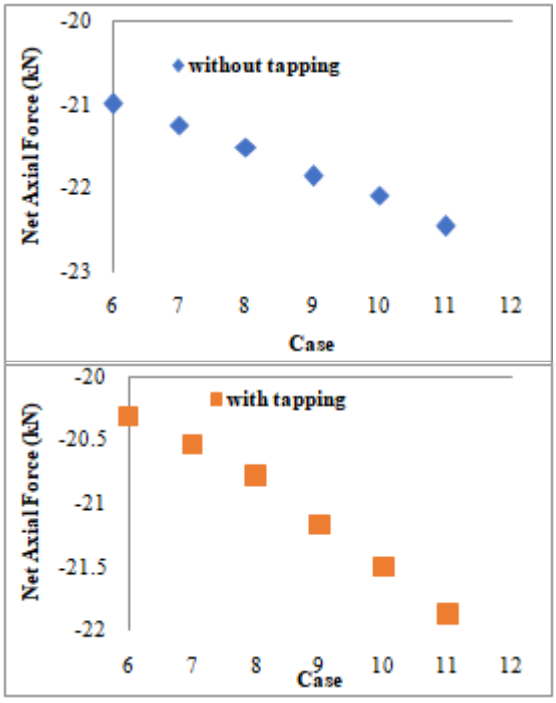

Figure 9: Net axial force in two layer LV winding for different effective axial height of LV winding keeping the height of HV winding fixed

5.3 Short Circuit Forces in HV Winding

(a) Average radial forces: The figure 10 gives the average radial force in HV winding for different effective axial height of one layer LV winding keeping the height of HV winding fixed.

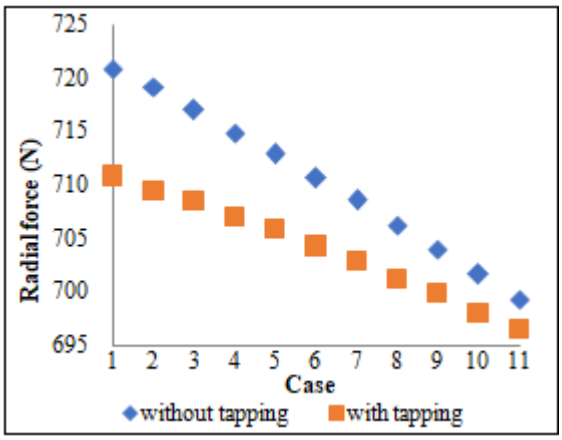

Figure 10: Average radial force in HV winding for different effective axial height of one layer LV winding keeping the height of HV winding fixed

As the effective height of LV winding relative to HV winding is decreased (Case-5 to Case-1) there is a marginal increase in the magnitude of radial force in HV winding (directed towards the tank). As the effective height of LV winding relative to HV winding is increased (Case-7 to Case-11) the radial forces (directed towards the tank) decreases marginally. The presence of tapping reduces the value of average radial force marginally, with relatively more effect in Case-1 and least in Case-11

(b) Net axial forces: The figure 11 gives the net axial force in HV winding for different effective axial height of one layer LV winding keeping the height of HV winding fixed.

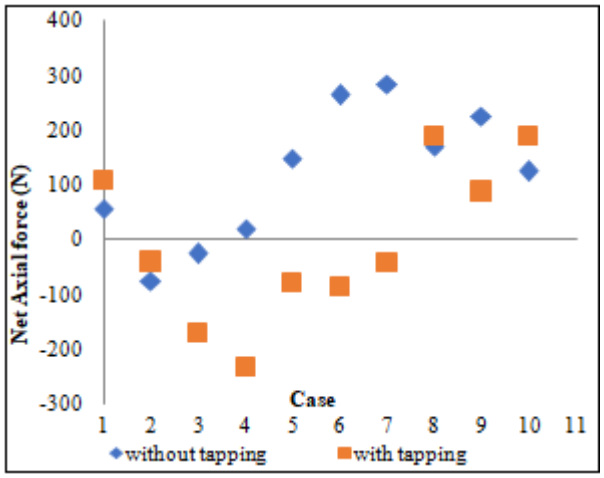

Figure 11: Net axial force in HV winding for different effective axial height of one layer LV winding keeping the height of HV winding fixed

The least magnitude of axial force directed towards the upper yoke for untapped condition is for Case-4, Case-1, Case-10, Case-5, Case-8, Case-9, Case-7, Case-6 and Case-11 (in that order). The least magnitude of net axial force directed toward the lower yoke for untapped condition is for Case-3, and Case-2 (in that order). The least magnitude of net axial force directed toward the upper yoke for tapped condition is for Case-9, Case-1, Case-10 and Case-8 (in that order), The least magnitude of net axial force directed toward the lower yoke for tapped condition is for Case-7, Case-2, Case-5, Case-6, Case-3, and Case-4 (in that order).

5.3.1 Short circuit forces in HV winding when LV winding is two layer type

*(a) Average radial forces:*The figure12 gives the average radial force in HV winding for different effective axial height of two layer LV winding keeping the height of HV winding fixed. As the effective height of LV winding compared to HV winding is increased (Case-7 to Case-11), there is a marginal decrease in the magnitude of radial force. The presence of tapping reduces the value of average radial force marginally.

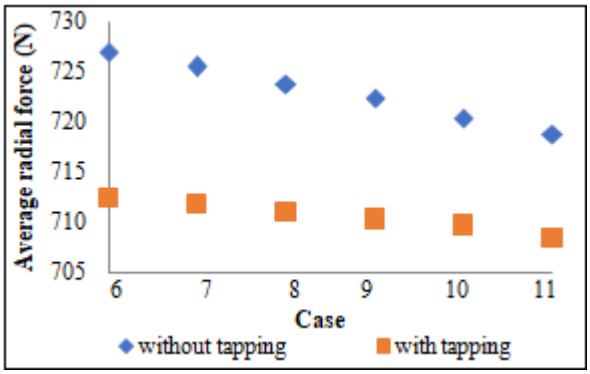

Figure 12: Average radial force in HV winding for different effective axial height of two-layer LV winding keeping the height of HV winding fixed

(b)Net axial forces: The figure13 gives the net axial force in HV winding for different effective axial height of two layer LV winding keeping the height of HV winding fixed.

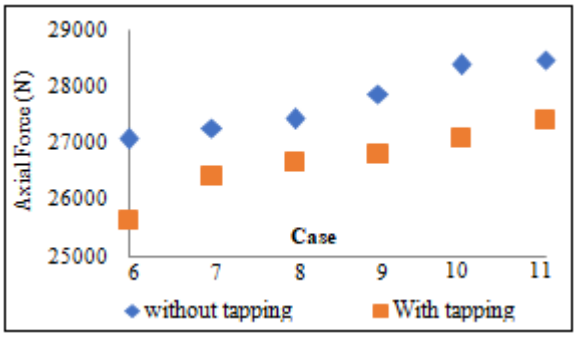

Figure 13: Net axial force in HV winding for different effective axial height of two-layer LV winding keeping the height of HV winding fixed

As the effective height of LV winding becomes more than the height of HV winding the magnitude of net axial force directed upwards towards the upper yoke increases. The presence of tapping reduces the magnitude of the upwards directed axial force.

6. Conclusion

For a LV winding of one-layer helical type the force developed in both the LV and HV windings are of torsional nature, hence so as to have least magnitude of net axial force in LV and HV windings the effective height of the LV winding should preferably be 2% more than the height of HV winding. For a center tapped design so as to have least magnitude of net axial force in LV and HV windings the effective height of the LV winding should preferably be 1% more than the height of HV winding.

For a LV winding is two-layer helical type, the radial force in the outer layer is 3 times that in the inner layer and the axial force in the outer and inner layer are equal. The net axial force in the LV winding is directed downwards towards the lower yoke and in HV winding the axial force is directed towards the upper yoke. To have least magnitude of net axial force in LV and HV windings the effective height of the LV winding should preferably be equal to the height of HV winding.

References

[1] Salon S, LaMattian B, and Sivasubramaniam K, (2000), "Comparison of Assumptions in Computation of Short Circuit Forces in Transformers," *IEEE Transaction on Magnetics*, 36(5), pp. 3521-3523.
[2] Wang H and Butler K L, (2001), "Finite Element Analysis of Internal Winding faults in Distribution Transformer," *IEEE Transactions on Power Delivery*, 16(3), pp. 422-428.
[3] Steurer M, and Frohlich K,(2002), "The Impact of Inrush Current on Mechanical Stresses of High Voltage Power Transformer Coils," *IEEE Transactions on Power Delivery* , 17(1), pp. 155-160.
[4] Schmidt E, and Hamberger P, (2004), "Finite Element Analysis in Design Optimization of Winding Support and Tank Wall of Power Transformer," *International Conference on Power System Technology*, (2), pp. 1375-1380.
[5] Heydari H, Pedramrazi S M, and F Feghihi, (2007) "Mechanical Forces Simulation of 25kA Current Injection Transformer with Finite Element Method," *Proceedings of 7th International Power Engineering Conference*, (2), pp. 629-633.
[6] Faiz J, Ebrahimi B M, and Noori T,(2008) "Three and Two Dimensional Finite-Element Computation of Inrush Current and Short-Circuit Electromagnetic Forces on Windings of a Three-Phase Core-Type Transformer," *IEEE Transactions on Magnetics*, 44(5), pp. 590-597.
[7] A da Costa, Sanz-Bobi M A, Rouco L, Palacios R, Flores L, and Cirujano P, (2011) "A Tool for the Assessment of Electromagnetic forces in Power Distribution Transformers," *Journal of Energy and Power Engineering*, 5(10), pp. 972-977.
[8] Kumbhar G B, and Kulkarni S V, (2007), "Analysis of Short-Circuit Performance of Split-Winding Transformer using Coupled Field-Circuit Approach," *IEEE Transactions on Power Delivery*, 22(2), pp. 936-942.
[9] Strac L, Kelemen F, and Zarko D, (2008), "Analysis of Short Circuit Forces at the Top of Low Voltage U Type and I Type Winding in A Power Transformer," *Proceedings of 13th Conference on Power Electronics and Motion Control*, pp. 855-858.
[10] Bakshi A, and Kulkarni S V, (2012), "Towards Short-Circuit Proof Design of Power Transformers," *International Journal for Computation and Mathematics in Electrical and Electronics Engineering*, 31(2), pp. 692-702.
[11] Ahn S M, Oh Yeon-Ho, Kim J K, Song J S, and Hahn S C, (2012), "Experimental Verification of Short-Circuit Electromagnetic Force for Dry Type Transformer," *IEEE Transactions on Magnetics*, 48(2), pp. 819-822.
[12] Deepika Bhalla, PhD thesis, "Identification of Transformer Incipient Faults using Artificial Intelligence Techniques."
[13] Chao Y, Wang X, and Dexin X, (2001) "Positive and Contrary-Direction Transposition of Double Helical Winding in Power Distribution Transformer," Proceedings of 5th International Conference on Electrical Machines and Systems, 1, pp. 198-200.
[14] Wang X, Yu S, Zhao Q, Wang S, Tang R, and Yuan X, (2003), "Effect of Helical Angle of Winding in Large Power Transformer," *Proceedings of International Conference on Electrical Machines and Systems*, 1, pp. 355-357.
[15] Deepika Bhalla, Raj Kumar Bansal, Hari Om Gupta, "Analyzing Short Circuit Forces in Transformer with Single Layer Helical LV Winding using FEM," *IEEE International Conference on Recent Advances in Engineering and Computational Sciences*, , 21st-22nd December 2015.
[16] Deepika Bhalla, R.K. Bansal, and H.O. Gupta, "Analyzing Short Circuit Forces in Transformer for Double Layer Helical LV Winding using FEM." *International Journal of Performability Engineering*, Vol. 14, no. 3, March 2018, pp. 425-433.
[17] Bianchi Nicola, "Electrical Machines Analysis Usieng Finite Elements, Taylor and Francis Group, CRC Press, 2005
[18] Clause 16.11.2 of *IS- 2026*, Standards and Specifications of Power Transformer.
[19] IEC standard 60076 Power Transformers
[20] Harlow J H, Electrical Power & Transformer Engineering, CRC Press.
[21] Kulkarni S V, and Khapaarde S A, Transformer Engineering: Design and Practice, New York:Marcel Dekker, May 2004.
[22] Meeker David, Finite Element Method Magnetics, Version 4.2, Users Manual, 201